# BEAM DYNAMIC STUDY OF HIGH INTENSITY LINAC FOR THE NEUTRON SCIENCE PROJECT AT JAERI

K. Hasegawa, H. Oguri, Y. Honda*, H. Ino*, M. Mizumoto and R. A. Jameson**
Japan Atomic Energy Research Institute, Tokai-mura, Ibaraki-ken, 319-1195, Japan
*Mitsubishi Heavy Industries, Ltd., Nagoya-shi, Aichi-ken, 455-8515, Japan
**Los Alamos National Laboratory, Los Alamos, NM, 87545, USA

*Abstract*

Beam dynamics study of a high intensity proton linac has been performed for the Neutron Science Project at JAERI. The RFQ parameters are designed by using the RFQUIK code. An equipartitioned design approach is taken for the DTL, the SDTL and the superconducting linac sections. The linac parameters and the results of the beam dynamics study are presented.

## 1 INTRODUCTION

A high intensity proton linear accelerator with an energy of 1.5 GeV and an average beam power up to 8 MW has been proposed for the Neutron Science Project (NSP) at JAERI [1].

The linac system design and the beam dynamics study are carried out considering the following issues.

1) The linac should have the lower beam emittance to prevent activation, and

2) The linac should be operated in both pulse and CW modes to meet the various experimental requirements.

Table 1. Operation mode of the NSP Linac

| Operation Mode | Pulse | | | CW |
|---|---|---|---|---|
| Beam Energy (GeV) | 1.5 | | | 1.5 |
| Repetition (Hz) | 50 | | | CW |
| Accelerated Particle | H- | | H+ | H+ |
| | Phase1 | Phase2 | Phase2 | |
| Peak Current (mA) | 16.7 | 30 | 30 | 5.3 |
| Pulse Width (msec) | 2 | 3.7 | 2.2 | CW |
| Beam Power (MW) | 1.5 | 5 | 3 | 8 |

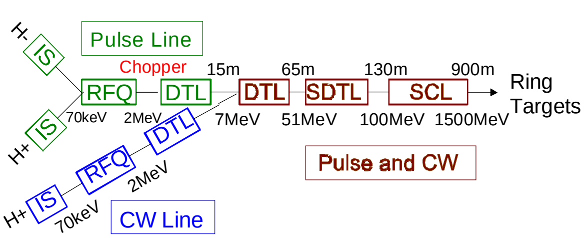


Figure 1. A schematic drawing of the linac system

## 2 LINAC SYSTEM DESIGN

The operation mode of the NSP linac and a schematic drawing of the system are shown in Table 1 and Figure 1, respectively. The linac has some accelerator subsystems: RFQ, DTL, separated-type DTL (SDTL) and superconducting linac (SCL).

The duty factors of the pulse operation and the CW operation are different by several times, but on the contrary, the peak beam currents are also different by several times. This beam current difference is not narrow enough for optimum operation in a single RFQ. In addition to that, for the pulse operation, the intermediate pulsing choppers for the ring injection have to be installed, whereas no choppers are required for the CW operation. Based on the above reasons, injector lines for the pulse operation and for the CW operation are optimized separately, and the two lines merge in the DTL section at 7 MeV.

The SDTL structure[2] is adopted for the higher energy DTL region because of some advantages such as the simpler structures and the smoother matching properties to the following section.

The superconducting linac (SCL) is a main option between 100 and 1500 MeV, because the characteristics of the cavities are suitable for the high duty factor operation and less beam loss will be expected due to the large bore size.

## 3 EQUIPARTITIONING DESIGN

For the system design of the DTL, the SDTL and the SCL sections, the equipartitioning design approach[3] is taken to reduce the emittance growth.

Wave number $k_{z0}$ for the longitudinal oscillation with \`n\`-rf gaps at zero current is

$$k_{zo} = \left[ -\frac{q}{mc^2} \frac{2\pi}{\lambda} \frac{1}{\beta_0^3 \gamma_0^3} \frac{1}{L_{total}} \sum_{k=1}^{n} \left\{ E_{0k} L_k \left( T_k \sin\phi_k + S_k \cos\phi_k \right) \right\} \right]^{1/2} \quad (1)$$

Using the following equipartitioning relation and the envelope equation[4] solves the wave number $k_{x0}$ for the transverse oscillation.

$$\gamma_0 \frac{\varepsilon_{nx}}{\varepsilon_{nz}} \frac{z_m}{a} = 1 \quad (2)$$

$$a \approx \left[\left(\frac{3}{2}\right)^2 \frac{Nr_c}{\beta_0^2\gamma_0^2}\frac{1}{k_{z0}^2}\left(\frac{k_{x0}^2}{k_{z0}^2}+\frac{1}{2}\right)^{-2} + \left(\frac{\varepsilon_{nx}}{\beta_0\gamma_0 k_{x0}}\right)^{3/2}\right]^{1/3} \quad (3)$$

$$z_m \approx \left[\frac{3}{2}\frac{Nr_c}{\beta_0^2\gamma_0^5}\frac{1}{k_{z0}^2}\left(\frac{k_{x0}^2}{k_{z0}^2}+\frac{1}{2}\right) + \left(\frac{\varepsilon_{nz}}{\beta_0\gamma_0^3 k_{z0}}\right)^{3/2}\right]^{1/3} \quad (4)$$

where

$\beta_0$: v/c $\gamma_0$: Lorentz factor $\lambda$: RF wavelength
$\varepsilon_{nx}$, $\varepsilon_{nz}$: Normalized transverse and longitudinal emittances
$a$, $z_m$ : Radius and longitudinal half-length of ellipsoidal bunch, respectively
$N$: Number of particles in a bunch
$L_{total}$: Length of a focusing period

In the design, the Q magnet field gradients are adjusted to keep above equations.

## 4 RFQ DESIGN

### *4.1 Design Descriptions*

Two RFQs optimized for the higher and the lower beam currents have been designed to obtain better beam qualities, respectively. The higher current RFQ, operated in the pulse mode, is optimized at a beam current around 30 mA. The lower current RFQ is optimized below 10 mA. The RFQUIK and CURLI codes are used to design. The main parameters are listed in Table 2.

Relatively low peak fields are chosen for reliable and stable operation. The lower field leads to a longer RFQ, but less structure RF power loss density is suitable for the higher duty factor operations.
Figure 2 shows design parameters vs. length for the higher current and the lower current RFQs. In the design, we use a longer shaper section to obtain higher transmission rate and better emittance.

### *4.2 Simulation Results of the RFQs*

The beam simulation is performed with the PARMTEQ code. Figure 3 shows the transmission rate and the rms emittance for the higher and the lower current RFQs. More than 98 % transmission rate will be expected at the

Table 2 RFQ Parameters

| | Higher Current Pulse | Lower Current CW |
|---|---|---|
| Beam Current | 20 - 40 (mA) | ~7 (mA) |
| Energy | 0.07 - 2 (MeV) | 0.07 - 2 (MeV) |
| Frequency | 200 (MHz) | 200 (MHz) |
| Duty Factor | ~30 (%) | 100 (%) |
| Peak Field | 1.65 Ek | 1.5 Ek |
| Length | 3.58 (m) | 3.91 (m) |
| Structure RF Power | 325 (kW) | 300 (kW) |

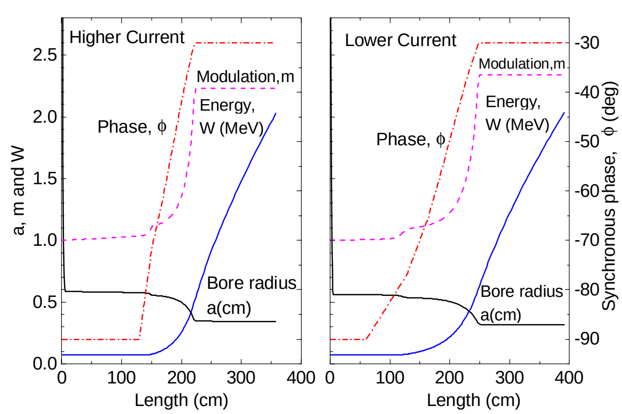


Figure 2. Design parameters for the higher and the lower current RFQs

beam current up to 40 mA and 15 mA for the higher and the lower current RFQs, respectively. The lower current RFQ has better longitudinal emittance up to 15 mA than the higher current RFQ, and vice versa above 20 mA.

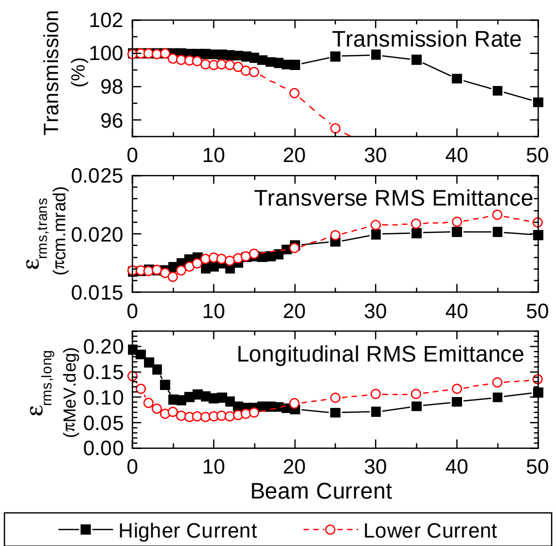


Figure 3. Transmission rate and normalized rms emittance for the higher and the lower current RFQs

## 5 DTL AND SDTL DESIGN

### *5.1 Design Descriptions*

The 200 MHz DTL follows the RFQ at 2 MeV. Up to 7 MeV, two DTLs are prepared for the pulse and the CW lines. The DTL accelerates protons up to 51 MeV and is followed by the SDTL. The lower $E_0$ of 1.5 MV/m is taken to reduce the heat dissipation of the structures. The lengths of the DTL and the SDTL are 57 m and 63 m, respectively

The SDTL structure is adopted from 51 to 100 MeV. The principles of the SDTL are very similar to those of the DTL, but the Q magnets are installed outside of the tank. As a beam dynamics design aspect, smoother transverse matching to the next section is expected, because the following SCL has a similar doublet focusing system.

### 5.2 Simulation Results

The equipartitioned design and the beam simulation are performed with the modified PARMILA code. The beam sizes in the simulation results are shown in Figure 4. There is an increase of the beam sizes both in the transverse and the longitudinal directions. The beam bunch keeps a nearly spherical shape in the DTL and the SDTL sections.

The rms and the 90 % emittance growth rates are about 7 % and 10 % at the highest, respectively. Further matching work is required to eliminate modulations of the beam sizes.

## 6 SUPERCONDUCTING LINAC

A schematic layout of the SCL is shown in Figure 5. The SCL is composed of 8 sections optimized for the phase slips due to the particle velocity and the cavity length difference. Each section has identical 5 cell cavities with surface peak field of 16 MV/m. Two cavities are laid in one doublet focusing period. The frequency is 600 MHz, which is 3 times of the lower energy sections. The total number of cavities is 284 and the length is 690 m. The detailed design and optimization study is described in Reference 5.

The designed wave numbers, the beam sizes and the equipartitioning factors are shown in Figure 6. The equipartitioning factor is defined by $\gamma_0(\varepsilon_{nx}/\varepsilon_{nz})(z_m/a)$, which is a left side of the equation (2). The design results at this stage show a decrease of wave numbers both in transverse and the longitudinal directions. There is a monotonous decrease of the longitudinal beam size, while slight increase of the transverse beam size. The beam size ratio $z_m/a$ has a dependence of $1/\gamma_0$ as expected in the equation (2). The equipartitioning factor around 0.9 obtained by the simulation results shows the design parameters are nearly equipartitioned: further work and better matching are expected to improve the performance.

The transverse and the longitudinal rms emittances are nearly constant or only 1% increase [5].

## 7 SUMMARY

Beam dynamics studies have been performed for the NSP linac. To meet the higher and the lower current operation modes with better beam emittance, two injector lines and optimized RFQs are designed. The equipartitioning design approach for the DTL, the SDTL and the SCL sections is taken to reduce the emittance growth. Further optimization study and matching work are expected to improve the performance.

## 8 REFERENCES


[1] M. Mizumoto et al.: 'A Proton Accelerator for the Neutron Science Project at JAERI', these proceedings.

[2] T. Kato: 'Proposal of a Separated-Type Proton Drift Tube Linac for a Medium-Energy Structure', KEK Report 92-10 (1992).

[3] R. A. Jameson: AIP Conference Proceedings 279, 969, 1993, ed. J.S. Wurtele.

[4] M. Reiser: 'Theory and Design of Charged Particle Beams', John Wiley & Sons, Inc., 1994

[5] Y. Honda et al.: 'A Conceptual Design Study of Superconducting Proton Linear Accelerator for Neutron Science Project', these proceedings.


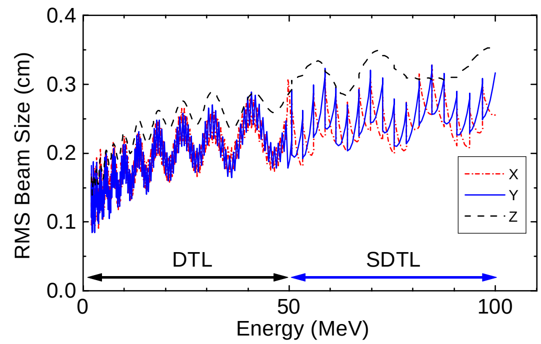


Figure 4. Beam sizes at the DTL and the SDTL

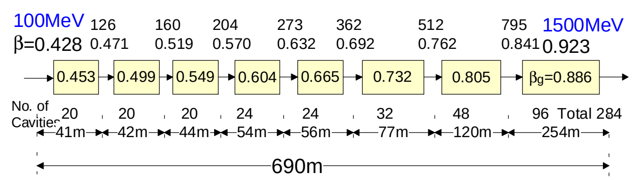


Figure 5. A schematic layout of the superconducting linac

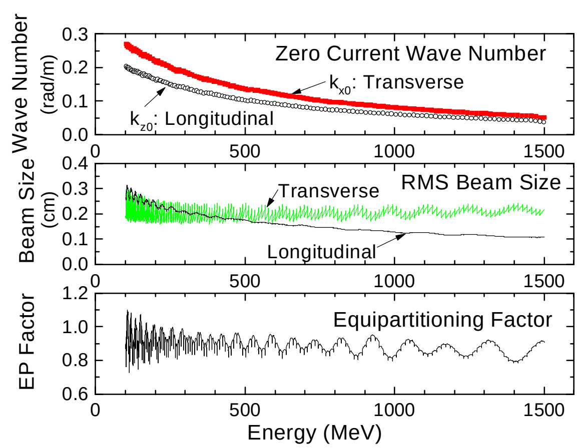


Figure 6. Design and beam simulation result of the superconducting linac section.